



Universiteit
Leiden
The Netherlands

Evaluating a phase-specific approach to aortic flow: a 4D flow MRI study

Ramaekers, M.J.F.G.; Westenberg, J.J.M.; Venner, M.F.G.H.M.; Juffermans, J.F.; Assen, H.C. van; Kiefte, B.J.C. te; ... ; Schalla, S.

Citation

Ramaekers, M. J. F. G., Westenberg, J. J. M., Venner, M. F. G. H. M., Juffermans, J. F., Assen, H. C. van, Kiefte, B. J. C. te, ... Schalla, S. (2023). Evaluating a phase-specific approach to aortic flow: a 4D flow MRI study. *Journal Of Magnetic Resonance Imaging*, 59(3), 1056-1067. doi:10.1002/jmri.28852

Version: Publisher's Version

License: [Creative Commons CC BY-NC 4.0 license](#)



Downloaded from: <https://hdl.handle.net/1887/3754516>

Note: To cite this publication please use the final published version (if applicable).

Evaluating a Phase-Specific Approach to Aortic Flow: A 4D Flow MRI Study

Mitch J.F.G. Ramaekers, MD,^{1,2,3,4*}  Jos J.M. Westenberg, PhD,⁴ 

Max F.G.H.M. Venner, MSc,² Joe F. Juffermans, MSc,⁴  Hans C. van Assen, PhD,⁴ 

Bastiaan J.C. te Kiefte, MD,⁴ Bouke P. Adriaans, MD, PhD,^{1,2}  Hildo J. Lamb, MD, PhD,⁴ 

Joachim E. Wildberger, MD, PhD,^{1,3} and Simon Schalla, MD, PhD^{2,3}

Background: Aortic flow parameters can be quantified using 4D flow MRI. However, data are sparse on how different methods of analysis influence these parameters and how these parameters evolve during systole.

Purpose: To assess multiphase segmentations and multiphase quantification of flow-related parameters in aortic 4D flow MRI.

Study Type: Prospective.

Population: 40 healthy volunteers (50% male, 28.9 ± 5.0 years) and 10 patients with thoracic aortic aneurysm (80% male, 54 ± 8 years).

Field Strength/Sequence: 4D flow MRI with a velocity encoded turbo field echo sequence at 3 T.

Assessment: Phase-specific segmentations were obtained for the aortic root and the ascending aorta. The whole aorta was segmented in peak systole. In all aortic segments, time to peak (TTP; for flow velocity, vorticity, helicity, kinetic energy, and viscous energy loss) and peak and time-averaged values (for velocity and vorticity) were calculated.

Statistical Tests: Static vs. phase-specific models were assessed using Bland–Altman plots. Other analyses were performed using phase-specific segmentations for aortic root and ascending aorta. TTP for all parameters was compared to TTP of flow rate using paired t-tests. Time-averaged and peak values were assessed using Pearson correlation coefficient. $P < 0.05$ was considered statistically significant.

Results: In the combined group, velocity in static vs. phase-specific segmentations differed by 0.8 cm/sec for the aortic root, and 0.1 cm/sec ($P = 0.214$) for the ascending aorta. Vorticity differed by $167 \text{ sec}^{-1} \text{ mL}^{-1}$ ($P = 0.468$) for the aortic root, and by $59 \text{ sec}^{-1} \text{ mL}^{-1}$ ($P = 0.481$) for the ascending aorta. Vorticity, helicity, and energy loss in the ascending aorta, aortic arch, and descending aorta peaked significantly later than flow rate. Time-averaged velocity and vorticity values correlated significantly in all segments.

Data Conclusion: Static 4D flow MRI segmentation yields comparable results as multiphase segmentation for flow-related parameters, eliminating the need for time-consuming multiple segmentations. However, multiphase quantification is necessary for assessing peak values of aortic flow-related parameters.

Level of Evidence: 2

Technical Efficacy Stage: 3

J. MAGN. RESON. IMAGING 2024;59:1056–1067.

Three-dimensional and three-directional phase-contrast MRI, also known as 4D flow MRI, is used for visualizing aortic blood flow.¹ Hemodynamic markers, including wall shear stress, vorticity, helicity, and energy loss can be quantitatively determined from 4D flow MRI velocity data.¹ These flow-related parameters have been assessed during follow up

View this article online at wileyonlinelibrary.com. DOI: 10.1002/jmri.28852

Received Nov 30, 2022, Accepted for publication May 27, 2023.

*Address reprint requests to: M.J.F.G.R., Department of Radiology and Nuclear Medicine, Maastricht University Medical Center+, P. Debyelaan 25, 6229 HX, Maastricht, The Netherlands. E-mail: mitch.ramaekers@mumc.nl

Contract grant sponsor: Dutch Heart Foundation; Contract grant number: CVON-2017-08-RADAR.

From the ¹Department of Radiology and Nuclear Medicine, Maastricht University Medical Center+, Maastricht, The Netherlands; ²Department of Cardiology, Maastricht University Medical Center+, Maastricht, The Netherlands; ³Cardiovascular Research Institute Maastricht (CARIM), Maastricht, The Netherlands; and ⁴Department of Radiology, Leiden University Medical Center, Leiden, The Netherlands

This is an open access article under the terms of the [Creative Commons Attribution-NonCommercial](https://creativecommons.org/licenses/by-nc/4.0/) License, which permits use, distribution and reproduction in any medium, provided the original work is properly cited and is not used for commercial purposes.

of patients with aortic disease and may play a role monitoring progression of disease.^{2–6} Currently, there are several approaches to quantitative analysis of 4D flow MRI.^{3,6,7} To identify optimal methods, these need to be evaluated in a homogenous population at different time frames during the cardiac cycle. The first step in quantifying flow parameters is luminal segmentation, which comprises the conversion of volume, such as the ascending aorta, to 3D geometry. Luminal segmentations can be defined at one cardiac phase (or time step: static) or over multiple phases (phase-specific). For the aortic root and the ascending aorta, a phase-specific method could be the preferred method, due to the degree of aortic root displacement during systole.⁸ Static segmentation, however, allows faster analysis and could limit observer variation between segmentations, both considering the fact that less segmentations need to be performed.⁹ The influence of using phase-specific segmentations on the accuracy of quantified flow parameters is currently unclear. The second step in quantifying flow-related parameters is to calculate them within the volume defined by the luminal segmentation at, for example, peak flow or different time points during systole. However, data on the evolution of different flow-related parameters during systole is limited.¹⁰ Some studies have used time-averaged values (area under the curve), others have used peak values, and others have reported both.^{3,7,11,12} The agreement between these values has not been widely studied.

Thus the aims of this study were to: 1) compare multiple-phase to single-phase (static) segmentation in the aortic root and ascending aorta for the quantification of flow velocity and flow vorticity; 2) assess time to peak (TTP) values for various flow parameters (i.e., velocity, vorticity, helicity, kinetic energy, and viscous energy loss); and 3) compare time-averaged and peak values of flow parameters in healthy young volunteers and patients with ascending thoracic aortic aneurysms (aTAA).

Materials and Methods

The study was approved by the local medical ethical committees and all subjects provided written informed consent.

Study Population

Forty (20 male and 20 female) young (age 18–40 years) healthy volunteers (no history of cardiovascular disease, including aortic disease or connective tissue disease (chromosomal inherited syndromic aortic aneurysms), no contraindication for MRI, heart rate < 100 bpm, and blood pressure < 140/90 mmHg) were prospectively included at Maastricht University Medical Center + to obtain measurements and calculations in normal aortas.

To investigate whether the findings in young healthy individuals could also be observed in dilated aortas, 10 patients (7 male and 3 female) with aTAA were also included at Leiden University Medical Center.

MRI Acquisition

All subjects underwent imaging on a 3 T MR system (Philips Ingenia; Philips Healthcare, Best, the Netherlands) using the same scan-protocol. The velocity encoded turbo field echo 4D flow MRI sequence consisted of a full volumetric coverage of both left ventricular outflow tract and total aorta (including the iliac bifurcation). Details of the acquisition parameters are given in Table 1.

Images were acquired using navigator respiratory gating (using a 5 mm navigator window and one navigator per cardiac cycle), based on diaphragm excursion, and retrospective ECG gating. Velocity encoding was typically set at 150 cm/sec and adjusted if deemed necessary. Scan duration varied between 15 and 25 minutes, depending on heart rate and navigator efficiency. Left and right brachial blood pressure was measured directly after the MR examination while still in supine position.

Data Analysis

Analysis was performed by two readers (MR and MV, 4 and 1 years of experience), respectively (all segmentations were supervised by MR and adjusted if necessary) using commercially available (CAAS MR Solutions 5.2.1; Pie Medical Imaging, Maastricht, the Netherlands) and in-house developed software. Data analysis included phase-offset and aliasing correction prior to luminal segmentation. Semiautomatic segmentation was performed by CAAS MR Solutions as previously described and manually adjusted if deemed necessary.¹³ Segmentation of the aortic root and ascending aortic lumen was performed in all systolic cardiac phases with a sufficient velocity-to-noise ratio (determined by the assessor [MR]) (Fig. 1). Diastolic cardiac phases were not analysed due to the very low velocity-to-noise ratio and thus lack of contrast in the velocity maps. Since the aortic segments distal to the ascending aorta are

TABLE 1. 4D Flow MRI Parameters

FOV (mm)	450 × 298 × 68
Acquired voxel size (mm)	2.5 × 2.5 × 2.5
Reconstructed voxel size (mm)	1.41 × 1.41 × 2.5
Flip angle (°)	10
TE (msec)	2.7
TR (msec)	4.6
K-space segmentation factor	2
SENSE factor	2.5 (<i>P</i>) × 1.2 (<i>S</i>)
VENC (cm/sec)	150–175 ^a
(Reconstructed) cardiac phases	24–34
Temporal resolution (msec)	36.8

FOV, field of view; TE, echo time; TR, repetition time; VENC, velocity encoding.

^aOr higher in case of aortic valve stenosis in patients.

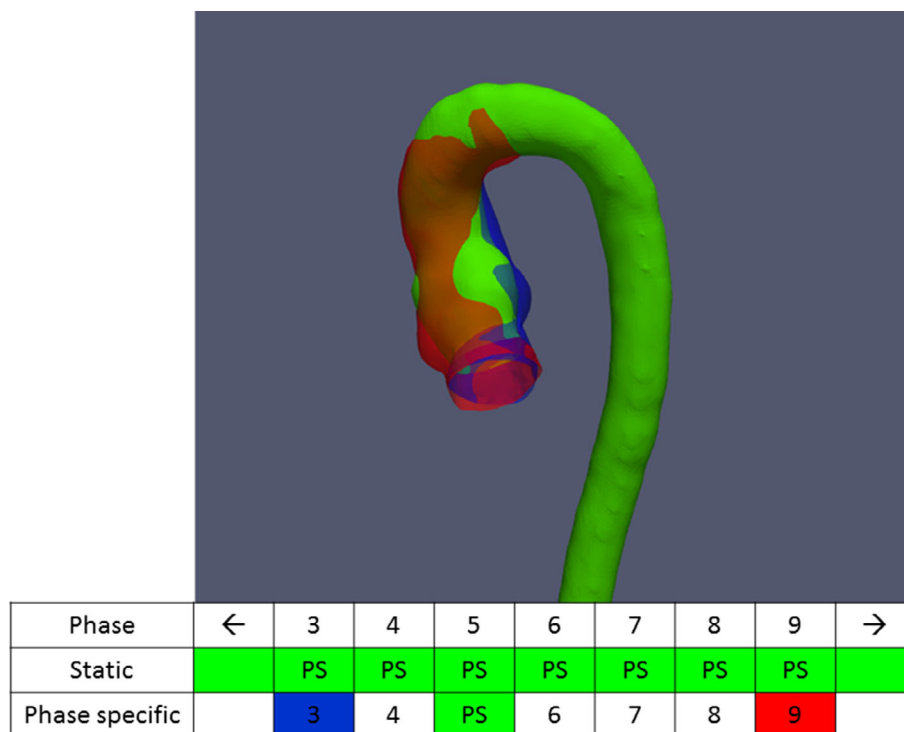


FIGURE 1: Aortic movement during the cardiac cycle. This figure illustrates the movement of the aortic root and ascending aorta during systole from 4D flow MRI images. The total aorta is segmented in peak systole (green). Other aortic root and ascending aorta segmentations for early systole (blue) and late systole (red) are superimposed. There is clear movement of these segments during the cardiac cycle. The table shows, which segmentation is used for the static (peak systole) and phase-specific methods (colors [green, blue, and red] correspond to those in the illustration). PS: peak systole.

considered to be static, one peak systolic segmentation was propagated to the other systolic phases for these segments. For the analysis of static segmentations of the aortic root and ascending aorta, the peak systolic segmentation (i.e., the phase with the highest flow rate) was propagated to the other systolic phases (Fig. 1). Seven planes were placed perpendicular to the centreline at the following anatomical locations: 1) aortic valve, 2) sino-tubular junction, 3) proximal to brachiocephalic trunk, 4) distal to the left subclavian artery, 5) diaphragm, 6) distal to the renal arteries, and 7) Proximal to the aortic bifurcation. By placing these planes, the aorta was divided into six segments: 1) aortic root (AoR), 2) ascending aorta (AAo), 3) Aortic arch (AoA), 4) descending aorta (DAo), 5) Supra-renal aorta (SRA), and 6) Infra-renal aorta (IRA) (Fig. 2). Analysis in patients with aTAA was limited to the AoR, AAo, AoA, and DAo since only the thoracic aorta was scanned. Maximum aortic diameters per segment were calculated automatically from the segmentation using in-house developed software. Flow-related parameters were calculated for each segment as averages per volume and per phase. Subsequently time-averaged and peak values, as well as TTP values, were obtained for all segments. Time-averaged values were calculated as the mean of 14 phases around the peak value (two highest phases, six before and six after). TTP was defined as milliseconds to peak value. The hemodynamic parameters that were evaluated during this study included flow rate, flow velocity, vorticity magnitude, absolute helicity, kinetic energy, and viscous energy loss.^{14,15} Vorticity and helicity were corrected for segment volume. Analysis of static vs. phase-specific segmentation and time-averaged vs. peak values were only performed for velocity and vorticity, as these parameters

form the basis for calculating other parameters. For example, kinetic energy is calculated from velocity, and helicity is calculated from vorticity. Static segmentations were only used for the static vs. phase-specific analysis. Other analyses were performed using the phase specific segmentations for aortic root and ascending aorta.

Statistical Analysis

Statistical analyses were performed using SPSS Statistics 25 (IBM, Armonk, NY). Continuous variables are presented as mean \pm standard deviation for normal distribution, or as median and interquartile range for skewed distribution. Categorical variables are presented as frequencies and percentages. TTP for all parameters was compared to TTP of flow rate using a paired *t*-test (separately for healthy volunteers and patients). Correlations between time averaged values and peak values (separately for healthy volunteers and patients) were analyzed using Pearson's correlation coefficient (or Spearman's rank correlation coefficient in case of skewness of the data). For the comparison of static vs. phase-specific models Bland Altman plots were used for the combined group of healthy volunteers and patients, with limits of agreement (LOA: mean \pm 1.96 standard deviations). A *P*-value of <0.05 was considered statistically significant.

Results

Demographics

The mean age of the 40 healthy volunteers was 28.9 ± 5.0 years. Mean systolic blood pressure was 120.2 ± 11.4 mmHg for the left arm and 120.7 ± 13.4 mmHg for the right arm. Mean

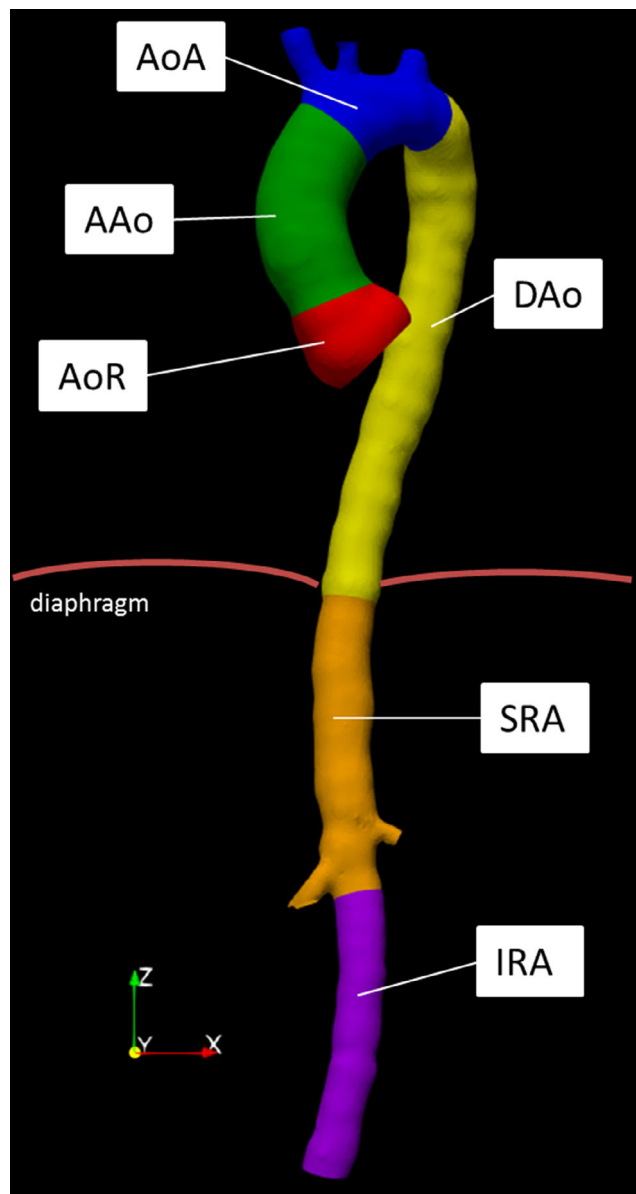


FIGURE 2: Anatomical segments assessed in this study. AoR: aortic root; AAO: ascending aorta; AoA: aortic arch; DAAo: descending aorta; SRA: supra-renal aorta; IRA: infra-renal aorta.

diastolic blood pressure was 71.4 ± 7.4 mmHg for the left arm and 68.8 ± 6.6 mmHg for the right arm. The mean age for the 10 patients was 54 ± 8 years. Six patients had degenerative aortic aneurysms, three patients had connective tissue disease, one patient had a bicuspid aortic valve related aortopathy, and one patient with aneurysm had both a bicuspid aortic valve and connective tissue disease. Aortic diameters for all segments are reported in Table 2.

Static- vs. Phase-Specific Segmentation

Bland–Altman plots of pairs of measurements from static- vs. phase-specific segmentations with mean differences and limits of agreement for the total group (healthy volunteers and patients) are shown in Fig. 3a–d. Mean differences for

TABLE 2. Aortic Diameters (mm)

	Males <i>n</i> = 20	Females <i>n</i> = 20	Total <i>n</i> = 40	Patients <i>n</i> = 10
AoR	33 ± 3	30 ± 2	32 ± 3	45 ± 4
AAo	28 ± 2	26 ± 1	27 ± 3	44 ± 3
AoA	25 ± 2	25 ± 1	25 ± 2	34 ± 3
DAAo	22 ± 2	22 ± 1	22 ± 2	28 ± 4
SRA	19 ± 2	17 ± 1	18 ± 1	–
IRA	17 ± 1	15 ± 1	16 ± 2	–

Data presented as mean ± standard deviation. AoR: aortic root; AAO: ascending aorta; AoA: aortic arch; DAAo: descending aorta; SRA: supra-renal aorta; IRA: infra-renal aorta.

velocity were statistically significant in the AoR (0.8 cm/sec [LOA −3.7 to 5.2 cm/sec]) for the AoR. Mean differences for velocity in the AAO were 0.1 cm/sec (LOA −2.3 to 2.6 cm/sec) for the AAO. Mean differences for vorticity magnitude were $167 \text{ sec}^{-1} \text{ mL}^{-1}$ (LOA −1675 to $2009 \text{ sec}^{-1} \text{ mL}^{-1}$) for the AoR and $59 \text{ sec}^{-1} \text{ mL}^{-1}$ (LOA −1088 to $1205 \text{ sec}^{-1} \text{ mL}^{-1}$; Table 3). Velocity measurements in the static segmentation showed a strong correlation with phase-specific segmentations in the AoR ($r = 0.975$) and AAO ($r = 0.995$). Vorticity measurements in the static segmentation also showed a strong correlation with phase-specific segmentations in the AoR ($r = 0.992$) and AAO ($r = 0.995$) (Table 3 and Fig. 4).

TTP in Healthy Volunteers

Peak flow arrived significantly later in each consecutive segment in healthy volunteers. Differences in TTP for flow rate in healthy volunteers were 16 ± 17 msec (AoR to AAO), 16 ± 19 msec (AAo to AoA), 30 ± 20 msec (AoA to DAAo), 9 ± 15 msec (DAAo to SRA), 32 ± 16 msec (SRA to IRA; Fig. 5a).

In the root, with respect to blood flow rate, vorticity, helicity, and energy loss all peaked significantly later (120 ± 20 msec vs. 129 ± 19 msec; 136 ± 30 msec; and 132 ± 31 msec, respectively). The largest differences in TTP were seen in the ascending aorta: with respect to blood flow, vorticity, helicity, and viscous energy loss peaked significantly later (136 ± 23 msec vs. 162 ± 35 msec; 168 ± 33 msec; and 169 ± 29 msec, respectively). In the arch, with respect to blood flow rate, vorticity, and helicity peaked significantly later (151 ± 25 msec vs. 164 ± 27 msec; and 183 ± 29 msec, respectively). In the DAAo, with respect to blood flow rate, helicity peaked significantly later (206 vs. 181 msec). The other parameters in the DAAo and the distal segments (SRA and IRA) also showed significant, yet smaller, differences in

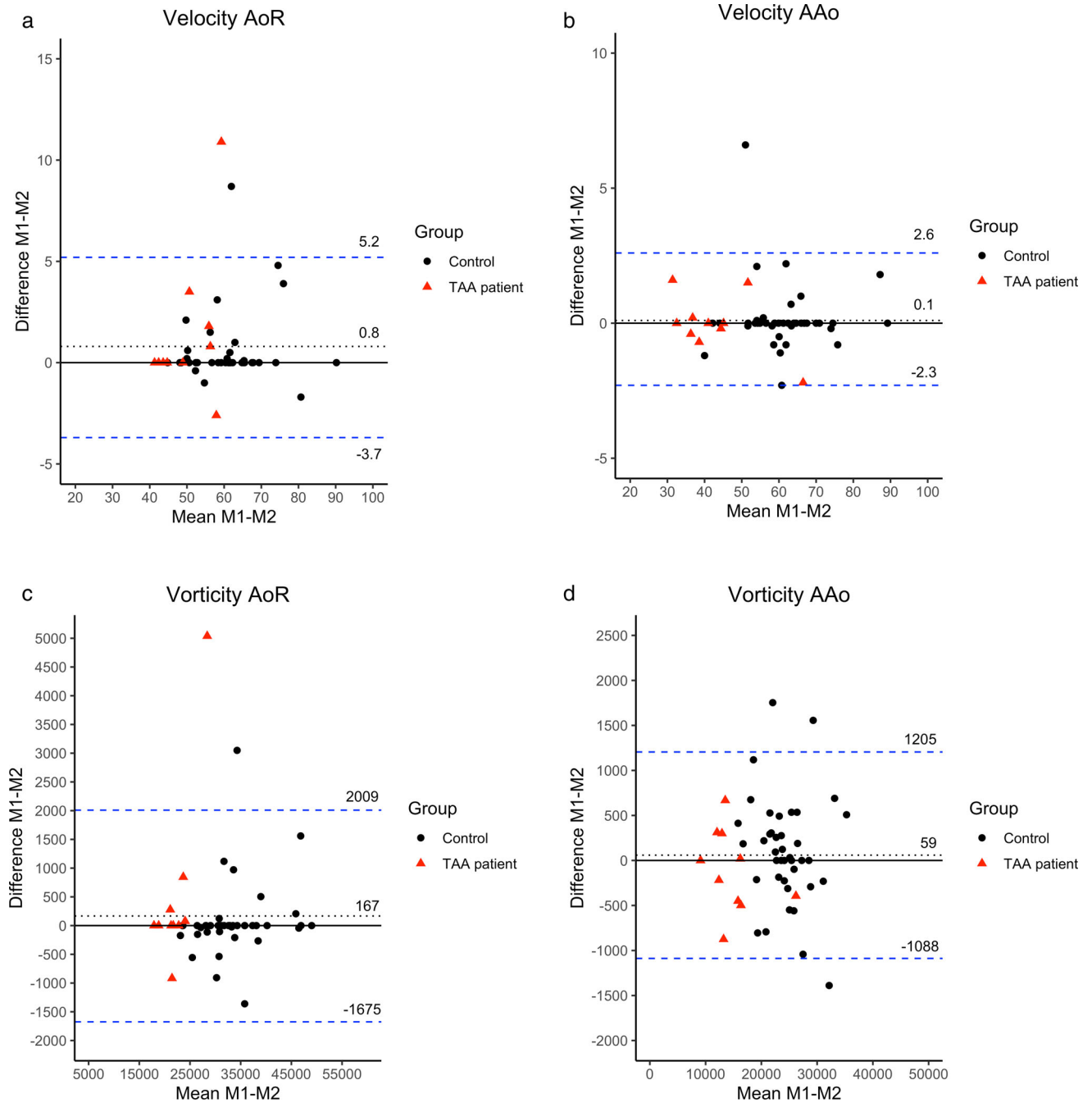


FIGURE 3: Phase-specific vs. static aortic models. The figures show Bland–Altman plots for differences in values for a phase-specific aortic model (M1) and a static aortic model (M2). Presented variables are velocity in the aortic root (a), ascending aorta (b), normalized vorticity in the aortic root (c), and ascending aorta (d). The blue line represents average differences, the red lines represent ± 1.96 standard deviations. Black dots represent healthy volunteers, red triangles represent patients.

TTP, which are presented in Table 4 and Fig. 5a. One example of flow visualization in multiple phases is presented in Fig. 6.

TTP in aTAA Patients

TTP values for patients are presented in Table 4 and Fig. 5b. There were significant differences in TTP for flow rate in consecutive segments in patients: 24 ± 28 msec (AoR to AAo), 7 ± 19 msec (AAo to AoA), and 16 ± 27 msec

(AoA to DAo; Fig. 5b). In the root, with respect to blood flow rate, helicity peaked significantly later (126 ± 33 msec vs. 144 ± 37 msec). In the ascending aorta, with respect to blood flow rate, velocity, vorticity, helicity, kinetic energy, and energy loss all peaked significantly later (150 ± 38 msec vs. 176 ± 54 msec; 205 ± 55 msec; 193 ± 51 msec; 178 ± 29 msec; and 204 ± 55 msec, respectively). In the aortic arch, with respect to blood flow rate, only helicity peaked significantly later (157 ± 47 msec vs. 189 ± 61 msec).

TABLE 3. Phase-Specific (M1) vs. Static Segmentation (M2)

	Paired <i>t</i> -test M1-M2 difference	<i>P</i> -value	Correlation coefficient M1-M2	<i>P</i> -value	Correlation coefficient differences – means	<i>P</i> -value
Velocity AoR (cm/sec)	0.8 ± 2.3	0.021*	0.975	<0.001*	0.076	0.598
Velocity AAo (cm/sec)	0.1 ± 1.26	0.214	0.995	<0.001*	−0.049	0.733
Vorticity AoR (sec ^{−1} mL ^{−1})	167 ± 940	0.468	0.992	<0.001*	0.073	0.612
Vorticity AAo (sec ^{−1} mL ^{−1})	59 ± 82	0.481	0.995	<0.001*	−0.020	0.889

AoR: aortic root; AAo: ascending aorta; M1: phase-specific aortic model; M2: static aortic model.

**P* < 0.05.

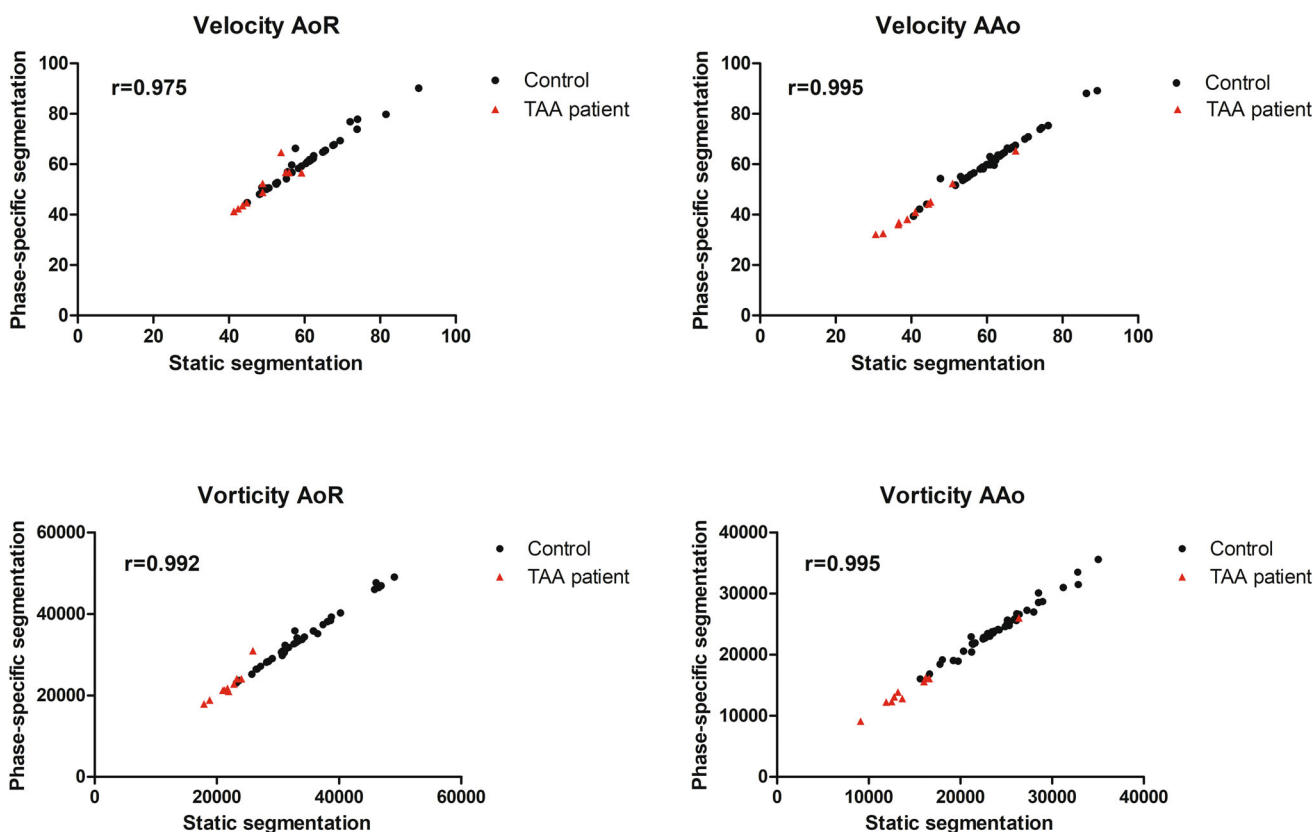


FIGURE 4: Correlation between values calculated in phase-specific and static aortic models. The figure shows the scatter plots and correlation coefficients for velocity (cm/sec) and normalized vorticity (sec^{−1} mL^{−1}) in the AoR and AAo. All correlations are statistically significant. Black dots represent healthy volunteers, red triangles represent patients.

One example of flow visualization in multiple phases is presented in Fig. 6.

Time Averaged vs. Peak Values in Healthy Volunteers

Time-averaged values for velocity and vorticity correlated strongly with peak-values for each segment in healthy volunteers (Fig. 7a). Time-averaged and peak velocity values in healthy volunteers correlated very strongly for AoR (*r* = 0.827), AAo

(*r* = 0.833), AoA (*r* = 0.787), DAo (*r* = 0.813), SRA (*r* = 0.863), and IRA (*r* = 0.880). Time-averaged and peak vorticity correlation was very strong for AoR (*r* = 0.928), AAo (*r* = 0.887), AoA (*r* = 0.891), DAo (*r* = 0.930), SRA (*r* = 0.940), and IRA (*r* = 0.941).

Time Averaged vs. Peak Values in Patients

Time-averaged values for velocity and vorticity correlated strongly with peak-values for each segment in patients

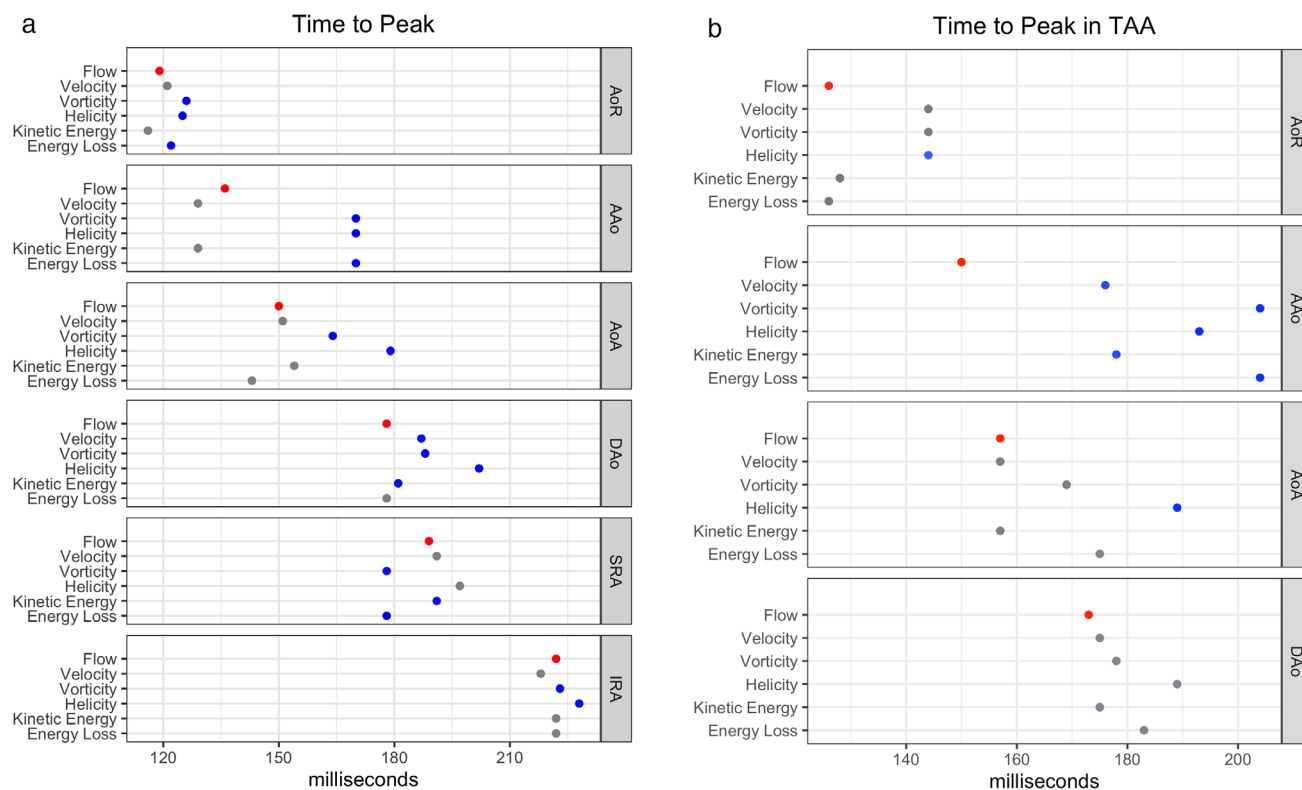


FIGURE 5: Mean TTP for flow parameters per segment for healthy volunteers (a) and patients (b). Red dots represent TTP for blood flow rate. Blue dots represent significant differences in TTP as compared to flow rate TTP. AoR: aortic root; AAO: ascending aorta; AoA: aortic arch; DAo: descending aorta; SRA: supra-renal aorta; IRA: infra-renal aorta.

(Fig. 7b). Time-averaged and peak velocity values in patients correlated very strongly for AoR ($r = 0.860$), AAO ($r = 0.858$), AoA ($r = 0.888$), and DAo ($r = 0.946$). Time-averaged and peak vorticity correlation was very strong for AoR ($r = 0.961$), AAO ($r = 0.946$), AoA ($r = 0.955$), and DAo ($r = 0.982$).

Discussion

In this observational study in healthy young volunteers and aTAA patients, multi-phase multi-segmentation approaches for aortic 4D flow MRI analysis were evaluated. Assessment of flow-related parameters during systole was performed with phase-specific segmentations for aortic root and ascending aorta considering their systolic displacement and with static segmentations for all other aortic segments. Diastole was not analyzed considering the low flow velocities and thus low velocity-to-noise ratio. The main conclusions of this study were: 1) a static single-phase segmentation of the aortic root and ascending aorta in peak systole resulted in similar quantitative values of velocity and vorticity as compared to a multiphase segmentation in healthy young volunteers and patients. Only for the AoR, differences were statistically significant (but small); 2) the flow peak occurred later in distal segments as compared to proximal segments; 3) in healthy volunteers, vorticity and helicity peaked significantly later

than flow in most segments, especially in the AAO, AoA, and DAo; in patients, similar trends were seen; and 4) peak values and time averaged values correlated strongly in both healthy volunteers and aTAA patients. Additionally, this study in a homogenous group of healthy young volunteers and a small group of aTAA patients might offer perspective in predicting aortic disease by assessing the systolic evolution of quantified flow-related parameters.

It takes time for the pulse wave created by left ventricular contraction to propagate along the aorta. The pulse wave velocity (PWV) reflects this phenomenon, and represents the propagation speed of the pulse.¹⁶ When the aorta stiffens, propagation times shorten^{17,18} and thus PWV will increase. The dynamic properties of 4D flow MRI allow analysis at each cardiac phase, with a 4D flow scan generally consisting of 25–35 phases, generating time-dependent results of aortic blood flow. Some of the results of this study, describing the delay in peak flow from proximal to distal aorta, may seem rather obvious. However, they are useful as they indicate which phases should be included in the analysis of peak values for flow-related parameters at specific segments. Segmental analysis of all flow-related parameters also showed a wide time range for parameters to peak within a single segment. In the ascending aorta, for example, vorticity, helicity, and energy loss peak 76–90 msec later as compared to blood flow rate. This means that, even for single anatomical

TABLE 4. TTP values as compared to TTP value for flow rate per segment in healthy volunteers (a) and patients (b).

	Flow rate TTP (msec)	Velocity TTP (msec)	P-value	Vorticity TTP (msec)	P-value	Helicity TTP (msec)	P-value	Kinetic Energy TTP (msec)	P-value	Viscous Energy Loss	P-value
(a) In healthy volunteers											
AoR	120 (±20)	124 (±19)	0.163	129 (±19)	0.001*	136 (±30)	<0.001*	117 (±25)	0.392	132 (±31)	0.004*
AAo	136 (±23)	131 (±20)	0.087	162 (±35)	<0.001*	168 (±33)	<0.001*	134 (±25)	0.524	169 (±29)	<0.001*
AoA	151 (±26)	155 (±26)	0.072	164 (±27)	<0.001*	183 (±29)	<0.001*	152 (±25)	0.871	148 (±29)	0.378
DAo	181 (±25)	185 (±23)	0.018*	188 (±25)	0.004*	206 (±31)	<0.001*	185 (±24)	0.045*	181 (±29)	0.963
SRA	190 (±26)	192 (±27)	0.085	185 (±28)	0.048*	199 (±33)	0.083	195 (±29)	0.013*	182 (±28)	0.005*
IRA	222 (±26)	220 (±26)	0.205	225 (±26)	0.045*	227 (±29)	0.027#	223 (±25)	0.407	225 (±25)	0.116
(b) Patients											
AoR	126 (±33)	144 (±33)	0.055	144 (±33)	0.055	144 (±37)	0.022*	129 (±22)	0.793	126 (±25)	0.956
AAo	150 (±38)	176 (±54)	0.010*	205 (±55)	<0.001*	193 (±51)	<0.001*	178 (±56)	0.017*	204 (±55)	<0.001*
AoA	157 (±47)	157 (±47)	–	169 (±62)	0.100	189 (±61)	0.003*	157 (±47)	–	175 (±76)	0.125
DAo	173 (±36)	175 (±52)	0.812	178 (±51)	0.601	189 (±61)	0.190	175 (±49)	0.715	183 (±46)	0.279

Data presented as mean ± standard deviation.
 AoR: aortic root; AAo: ascending aorta; AoA: aortic arch; DAo: descending aorta; SRA: supra-renal aorta; IRA: infra-renal aorta; TTP: time to peak; msec: milliseconds.
 *P < 0.05.

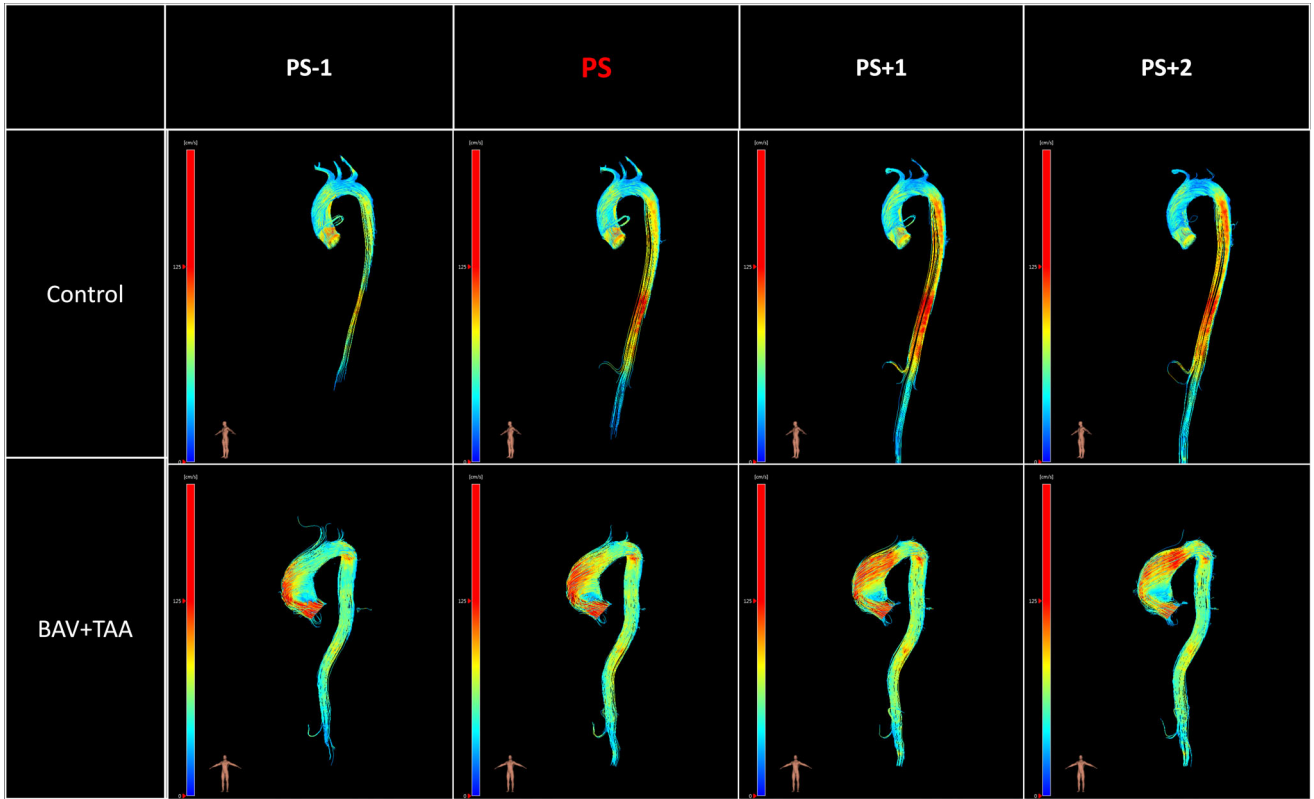


FIGURE 6: Streamline representation of aortic blood flow in a healthy volunteer (top row) and in a patient (bottom row). The figure shows streamlines in peak systole, one phase before, and two phases after peak systole. PS: peak systole; BAV: bicuspid aortic valve; TAA: thoracic aortic aneurysm.

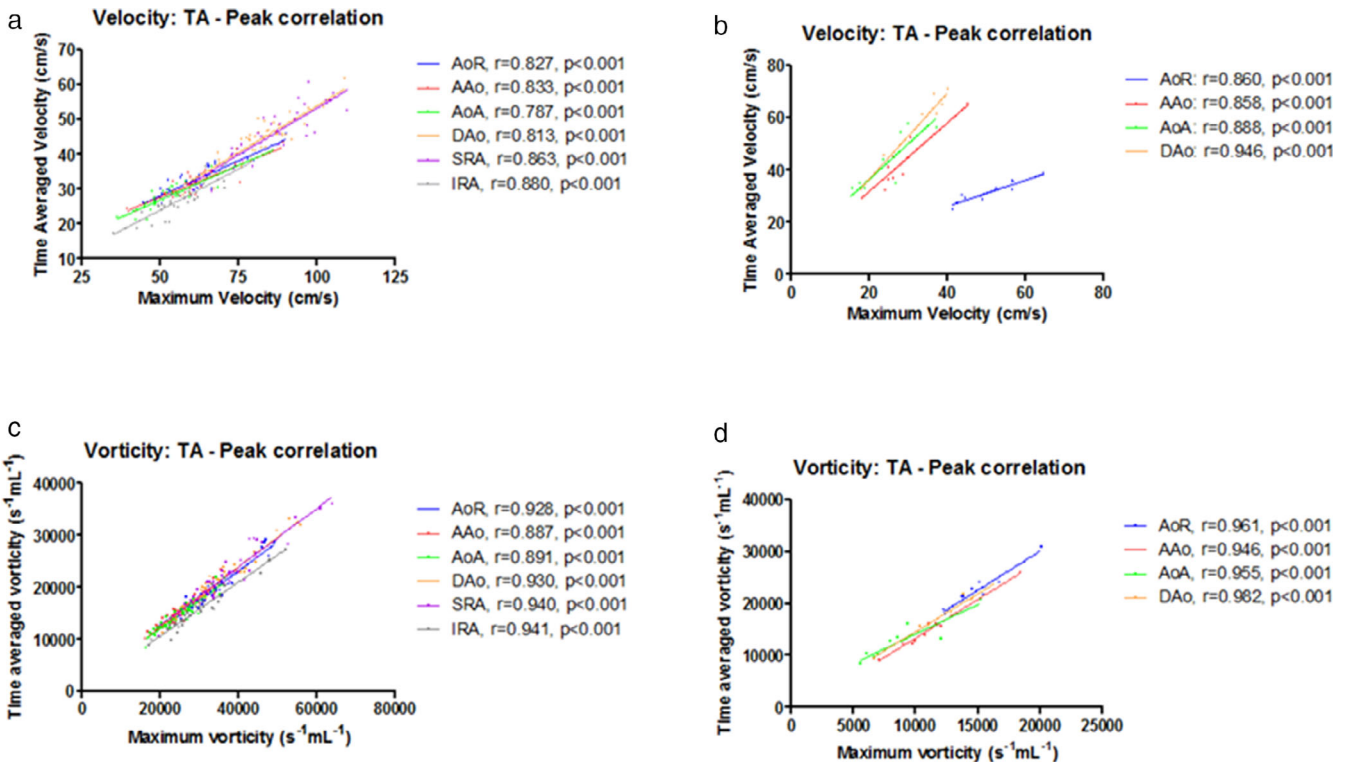


FIGURE 7: Correlations between time-averaged and peak velocity (a) and normalized vorticity (b) values for healthy volunteers and patients (c,d). The figure shows scatter plots and lines of best fit for velocity in healthy volunteers (a) and patients (c), and normalized vorticity in healthy volunteers (b) and patients (d) in all aortic segments. Corresponding correlation coefficients and P-values can be found in the legends. TA: time-averaged; AoR: aortic root; AAo: ascending aorta; AoA: aortic arch; DAo: descending aorta; SRA: supra-renal aorta; IRA: infra-renal aorta.

segments, multiple phases should be evaluated to obtain peak values. In this cohort, the necessary range of phases to find peak values for all parameters and all segments extended from -100 to 90 msec around peak systole.

The differences in TTP within a segment were found to be largest in the aortic arch and adjacent segments (AAo, AoA, and DAo). Kilner et al. described helical flow patterns in the aortic arch as early as 1993, using 4D flow MRI.¹⁹ Three stages of systolic flow in the aortic arch were described. The first stage, early systole, consists of high axial velocities that follow the shortest flow path, close to the inner curvature. During the second stage, more towards late systole when flow deceleration starts to occur, the axial velocity profile moves outwards, and secondary helical flow patterns develop. The third stage, end systole, reveals decreasing velocity, and more recirculating and rotational flow. The current study also showed delayed TTP for nonaxial velocities, which are related to helical flow patterns, and thus confirms earlier findings for quantified vorticity and helicity associated with secondary helical flow patterns that occur toward late systole in the AAo, AoA and DAo. These findings considering nonaxial velocities could also explain why kinetic energy peaks later than velocity (which appears unexpected since it is calculated from velocity).

Literature on TTP data is sparse. Burk et al., investigating 3D flow patterns in healthy volunteers, aged volunteers, and patients with aTAA, revealed differences in TTP velocity.⁷ Following these results, an interesting hypothesis is that changes in TTP occur before the actual flow deviates, and, therefore, could identify aberrant flow in an early stage: Assessing the dynamics of all flow parameters during the cardiac cycle may be helpful in recognizing flow disturbances at an early stage of aortic disease. Future studies could assess differences in TTP values in different age and patient groups.

Time-Averaged vs. Peak Values

Studies investigating aortic flow patterns have used time-averaged values, peak values, or both.^{3,7,11,12} The current study showed that there was a very strong correlation between peak values and time-averaged values in healthy volunteers and patients. Thus, quantification of peak values appears to be sufficient for clinical and research purposes. Limiting the analysis to the phases in which the peak is expected will reduce computational time for quantification of flow-related parameters compared to the full systolic quantification required for time-averaged values.

Static vs. Phase Specific Segmentations

In 4D flow analysis, the aortic volume needs to be determined from the luminal segmentation when normalizing quantified flow related parameters. However, a 4D flow consensus publication does not offer recommendations considering the luminal segmentation²⁰ and different methods have

been used.^{7,21} These include two dimensional (2D), static three-dimensional (3D) and phase-specific luminal segmentation. In two-dimensional (2D) segmentation, a 2D plane is placed, in which contours of the aortic lumen are drawn, and within this contour, through-plane calculations can be performed (e.g., flow velocity, WSS).⁷ To quantify regional or segmental values, 3D luminal segmentations are used. A 3D segmentation can be created for a single phase, after which the 3D model will be propagated to other phases for time-specific quantification of flow related parameters (static 3D segmentation³). A more time-consuming method is to perform phase-specific luminal segmentations and anatomical partitioning of the aorta, after which calculations per phase are performed within the corresponding segmentation.¹³

The static 3D luminal segmentation has been applied in several studies.^{3,22,23} Theoretically, it may be inaccurate considering the aortic movement during the cardiac cycle. As a result of left ventricular contraction, the aortic valve moves downward during systole, and returns to its original position during diastole.⁸ The aortic root and ascending aorta show a clockwise axial six-degree twist in addition to an 8.9 mm downward motion on average.²⁴ At the arterial ligament, between pulmonary artery and aorta, the aorta is considered fixed. Together with the fixed branches in the aortic arch, the aortic movement diminishes after the ascending aorta. Our study assessed the differences between static and phase-specific 3D models for the AoR and AAo, since these are the segments that displace most during the cardiac cycle. Only minimal differences in velocity were observed in the aortic root (although statistically significant in the aortic root, differences were small) and no differences were seen in the ascending aorta between static and phase-specific methods, with limits of agreement $<10\%$ of mean values. Differences in vorticity were also minimal between methods in the aortic root. In the ascending aorta, differences in vorticity between methods were present in almost all subjects but remained small. However, LAO were quite large relative to the mean vorticity. In general, these results correspond with the time-to-peak results in these segments. Since velocity and flow rate peak at approximately the same time, the phase in which it peaks matches with the phase in which the segmentation is made, which leads to no differences in most subjects. Vorticity, however, peaks significantly later than flow. Thus, the phase in which it peaks does not match with the segmentation phase for some cases, which leads to differences between static- and phase specific methods.

Acquisition and Processing Time in 4D Flow MRI

4D flow MRI requires long acquisition time and extensive image analysis in comparison with 2D flow. To develop a faster analysis method, this study assessed some of the processes in the analysis of 4D flow MRI. Based on the current study, analysis time can be substantially reduced since only a

single-phase (peak systole) needs to be segmented. While our quantification methods are almost fully automated, the segmentation is a semi-automatic process that requires manual input. Despite this, 4D flow MRI acquisition and post-processing remains a time-consuming task. With respect to the acquisition time, compressed sensing could accelerate acquisition.²⁵ With respect to postprocessing, recent studies have shown the potential of machine learning for both luminal segmentation and extraction of relevant flow-related parameters.^{26,27} These advances in acquisition and automatization of 4D flow MRI analysis, together with our contribution to a uniform analysis method, could reduce acquisition and postprocessing time.

Limitations

First, this study is mainly based on the data from relatively young, healthy volunteers. The results may not be translatable to all patients with aortic aneurysms or to elderly subjects with hypertension. Aortic flow is changed in patients with aortic aneurysms and may also change in elderly subjects,³ and timing of different flow-related parameters could therefore also be different. By incorporating a small sample of aTAA patients, we confirmed that patients showed similar results to those in healthy young volunteers.

Second, we did not perform an assessment of inter-reader reproducibility. Ideally, the results of this study would be confirmed by different readers.

Conclusion

In conclusion, single-phase, static segmentation does not result in significant differences in flow-related parameters compared to multiphase segmentation. However, multiphase quantification is required to assess time-to-peak values of aortic flow-related parameters.

Acknowledgements

We want to thank E.C. Nijssen, PhD for her contributions to this research article.

REFERENCES

1. Markl M, Schnell S, Wu C, et al. Advanced flow MRI: Emerging techniques and applications. *Clin Radiol* 2016;71(8):779-795.
2. Guala A, Dux-Santoy L, Teixido-Tura G, et al. Wall shear stress predicts aortic dilation in patients with bicuspid aortic valve. *JACC Cardiovasc Imaging* 2022;15(1):46-56.
3. Ramaekers MJFG, Adriaans BP, Juffermans JF, et al. Characterization of ascending aortic flow in patients with degenerative aneurysms: A 4D flow magnetic resonance study. *Invest Radiol* 2021;56(8):494-500.
4. Elbaz MSM, Scott MB, Barker AJ, et al. Four-dimensional virtual catheter: Noninvasive assessment of intra-aortic hemodynamics in bicuspid aortic valve disease. *Radiology* 2019;293(3):541-550.
5. Barker AJ, van Ooij P, Bandi K, et al. Viscous energy loss in the presence of abnormal aortic flow. *Magn Reson Med* 2014;72(3):620-628.
6. Ebel S, Kühn A, Aggarwal A, et al. Quantitative Normal values of helical flow, flow jets and wall shear stress of healthy volunteers in the ascending aorta. *Eur Radiol* 2022;32:8597-8607.
7. Burk J, Blanke P, Stankovic Z, et al. Evaluation of 3D blood flow patterns and wall shear stress in the Normal and dilated thoracic aorta using flow-sensitive 4D CMR. *J Cardiovasc Magn Reson* 2012;14:84.
8. Plonek T, Berezowski M, Kurcz J, et al. The evaluation of the aortic annulus displacement during cardiac cycle using magnetic resonance imaging. *BMC Cardiovasc Disord* 2018;18(1):154.
9. Juffermans JF, Westenberg JJM, van den Boogaard PJ, et al. Reproducibility of aorta segmentation on 4D flow MRI in healthy volunteers. *J Magn Reson Imaging* 2021;53(4):1268-1279.
10. Ha H, Ziegler M, Welander M, et al. Age-related vascular changes affect turbulence in aortic blood flow. *Front Physiol* 2018;9:36.
11. Frydrychowicz A, Stalder AF, Russe MF, et al. Three-dimensional analysis of Segmental Wall shear stress in the aorta by flow-sensitive four-dimensional-MRI. *J Magn Reson Imaging* 2009;30(1):77-84.
12. Trenti C, Ziegler M, Bjarnegård N, Ebbers T, Lindberger M, Dyverfeldt P. Wall shear stress and relative residence time as potential risk factors for abdominal aortic aneurysms in males: A 4D flow cardiovascular magnetic resonance case-control study. *J Cardiovasc Magn Reson* 2022;24(1):18.
13. van der Palen RLF, Roest AAW, van den Boogaard PJ, de Roos A, Blom NA, Westenberg JJM. Scan-rescan reproducibility of segmental Aortic Wall shear stress as assessed by phase-specific segmentation with 4D flow MRI in healthy volunteers. *Magma* 2018;31(5):653-663.
14. Kamphuis VP, Westenberg JJM, van der Palen RLF, et al. Scan-rescan reproducibility of diastolic left ventricular kinetic energy, viscous energy loss and vorticity assessment using 4D flow MRI: Analysis in healthy subjects. *Int J Cardiovasc Imaging* 2018;34(6):905-920.
15. Elbaz MS, van der Geest RJ, Calkoen EE, et al. Assessment of viscous energy loss and the association with three-dimensional vortex ring formation in left ventricular inflow: In vivo evaluation using four-dimensional flow MRI. *Magn Reson Med* 2017;77(2):794-805.
16. Westenberg JJM, de Roos A, Grotenhuis HB, et al. Improved aortic pulse wave velocity assessment from multislice two-directional in-plane velocity-encoded magnetic resonance imaging. *J Magn Reson Imaging* 2010;32(5):1086-1094.
17. Devos DG, Rietzschel E, Heyse C, et al. MR pulse wave velocity increases with age faster in the thoracic aorta than in the abdominal aorta. *J Magn Reson Imaging* 2015;41(3):765-772.
18. Westenberg JJ, Scholte AJ, Vaskova Z, et al. Age-related and regional changes of aortic stiffness in the Marfan syndrome: Assessment with velocity-encoded MRI. *J Magn Reson Imaging JMRI* 2011;34(3):526-531.
19. Kilner PJ, Yang GZ, Mohiaddin RH, Firmin DN, Longmore DB. Helical and retrograde secondary flow patterns in the aortic arch studied by three-directional magnetic resonance velocity mapping. *Circulation* 1993;88(5 Pt 1):2235-2247.
20. Dyverfeldt P, Bissell M, Barker AJ, et al. 4D flow cardiovascular magnetic resonance consensus statement. *J Cardiovasc Magn Reson* 2015;17(1):72.
21. Kauhanen SP, Liimatainen T, Kariniemi E, et al. A smaller heart-aorta-angle associates with ascending aortic dilatation and increases wall shear stress. *Eur Radiol* 2020;30(9):5149-5157.
22. Garcia J, Barker AJ, Collins JD, Carr JC, Markl M. Volumetric quantification of absolute local normalized helicity in patients with bicuspid aortic valve and aortic dilatation. *Magn Reson Med* 2017;78(2):689-701.
23. Sotelo J, Urbina J, Valverde I, et al. Three-dimensional quantification of vorticity and helicity from 3D cine PC-MRI using finite-element interpolations. *Magn Reson Med* 2018;79(1):541-553.
24. Beller CJ, Labrosse MR, Thubrikar MJ, Robicsek F. Role of aortic root motion in the pathogenesis of aortic dissection. *Circulation* 2004;109(6):763-769.

25. Ma LE, Markl M, Chow K, et al. Aortic 4D flow MRI in 2 minutes using compressed sensing, respiratory controlled adaptive K-space reordering, and inline reconstruction. *Magn Reson Med* 2019;81(6): 3675-3690.
26. Garrido-Oliver J, Aviles J, Córdova MM, et al. Machine learning for the automatic assessment of aortic rotational flow and wall shear stress from 4D flow cardiac magnetic resonance imaging. *Eur Radiol* 2022; 32(10):7117-7127.
27. Berhane H, Scott M, Elbaz M, et al. Fully automated 3D aortic segmentation of 4D flow MRI for hemodynamic analysis using deep learning. *Magn Reson Med* 2020;84(4):2204-2218.